INVESTIGATION OF OUTER LAYER SIMILARITY FOR ROUGH WALL BOUNDARY LAYERS

Karen A. Flack
Department of Mechanical Engineering
U.S. Naval Academy, Annapolis, MD, USA
flack@usna.edu

Michael P. Schultz
Jonathan S. Connelly
Department of Ocean Engineering
U.S. Naval Academy, Annapolis, MD, USA
mschultz@usna.edu

ABSTRACT

Based upon literature reviews, the papers of Jiménez (2004) and Flack *et al.* (2005) have concluded that changes to the turbulence structure across the boundary layer can be expected in rough wall flows where the boundary layer thickness (δ) is not much larger than the roughness height (k) or equivalent sand roughness height (k_s). The two studies state that outer layer similarity in the turbulence may cease to exist in cases where $\delta/k \leq 50$ or $\delta/k_s \leq 40$, respectively. In order to explore a limiting roughness height for boundary layer similarity, an experimental investigation was carried out on six rough surfaces representing two types of three dimensional roughness (sandpaper and woven mesh) in which $16 \leq \delta/k \leq 110$ and $6 \leq \delta/k_s \leq 91$. The measurements were conducted in a closed return water tunnel, over a momentum thickness Reynolds number (Re_θ) range of 6,100 to 13,000, using a two-component, laser Doppler velocimeter (LDV). The present results indicate that the mean velocity defect profiles for both the smooth and rough surfaces collapse well in both classic scaling and using the velocity scale of Zagarola & Smits (1998). The Reynolds stresses for all the surfaces collapse with smooth wall results outside of $3\text{-}4k_s$. These results indicate that turbulence similarity in the outer layer may be more robust than previously thought.

INTRODUCTION

The engineering importance of predicting the effect of wall roughness on boundary layer and pipe flows has been long been identified. Much of the seminal work in this area was carried out by Nikuradse (1933) and Colebrook & White (1937). Later investigations focused on the effect of roughness on turbulence structure (*e.g.* Perry & Joubert (1963); Perry *et al.* (1969); Antonia & Luxton (1971); Ligrani & Moffat (1986); Bandyopadhyay (1987)). An extensive review of the present knowledge of rough wall boundary layers is given by Raupach *et al.* (1991) and more recently by Jiménez (2004). Both, however, point out an overall lack in the understanding of the flow physics over rough walls. Accurate turbulence models also rely on the answers to some remaining fundamental questions with respect to the structure of rough wall boundary layers. These models treat roughness as a small perturbation to the smooth wall boundary layer. The question still remains as to whether or not there is similarity between rough and smooth boundary layers and if so what can be considered a small perturbation.

Hama (1954) proposed that the major effect of roughness on the mean velocity profile was a downward shift in the log-law region (ΔU^+) termed the roughness function, while the shape of the profile in the outer layer is unchanged. Numerous studies have observed a collapse of rough and smooth mean profiles in defect form, including the works of Bandyopadhyay (1987), Raupach, *et al.* (1991), Antonia & Krogstad (2001), Schultz & Flack (2003, 2005) and Flack *et al.* (2005). However, results from Krogstad *et al.* (1992) and Keirsbulck *et al.* (2002) indicate that the wake strength of the mean velocity profile is increased on rough walls, implying the effect of surface roughness may propagate well into the outer region. If this is the case, the application of rough wall models that rely on outer layer similarity will yield erroneous results.

The Reynolds number or wall similarity hypothesis of Townsend (1976) and subsequent extensions by Perry & Chong (1982) and Raupach *et al.* (1991) states that the turbulent stresses are independent of surface condition outside the roughness sublayer at sufficiently high Reynolds number when normalized by the wall shear stress. The underlying assumption to this hypothesis is that the boundary layer thickness (δ) is large compared to the roughness height (k). A number of studies have shown support for the wall similarity hypothesis including the works of Perry & Li (1990), Schultz & Flack (2003, 2005), and Flack *et al.* (2005). In contrast, Krogstad & Antonia (1994) noted that the turbulence structure is altered in the outer layer for rough walls. They also found that the near-wall turbulent motions for rough walls are inclined at a greater angle than for smooth walls. Such observations are important as they may lead to a better understanding of the nature of the inner layer/outer layer interaction. A possible explanation for the disparate findings may be due to the 'strong' roughness used in the investigations where effects were observed in the outer layer. A strong roughness here is defined as a surface whose equivalent sand roughness height (Schlichting (1979)), k_s, is a significant portion of the inner layer thickness (Schultz & Flack (2005)). This view is supported in the recent review article of Jiménez (2004). Strong roughness is found in engineering applications such as flows over gas turbine blades and in heat exchanger tubes. However, it is not indicative of many flows over ships and airplanes where thick boundary layers are present. A more clear definition of a strong roughness is needed to determine at what roughness height outer layer similarity fails, indicating that the roughness is no longer a small perturbation to the boundary layer.

The goal of the present research is to document fully-developed turbulent boundary layers on a range of three-dimensional rough surfaces for a range of roughness heights. Results will be presented for boundary layer measurements on flat plates covered with sandgrain and

woven mesh with δ/k varying from 16 to 110. To the authors' knowledge, this is the first study to measure turbulent stresses for such a large range of roughness heights for two very different roughness types in the same facility. The array of roughness heights were selected to span a range of surfaces from those that have previously displayed boundary layer similarity (the 80 grit sandpaper and the finest mesh, Flack *et al.* (2005)) to significantly rougher surfaces. From this, the similarity of both the mean velocity and turbulence structure on rough and smooth walls can be critically evaluated.

EXPERIMENTAL METHODS

The present experiments were conducted in the closed circuit water tunnel facility at the United States Naval Academy Hydromechanics Laboratory. The test section is 40 cm by 40 cm in cross-section and is 1.8 m in length, with a tunnel velocity range of 0 – 6.0 m/s. The current tests were run at a tunnel speed of ~2.0 m/s. (Re_x = 2.7 $\times 10^6$). Further details of the water tunnel facility are given in Schultz & Flack (2003). Seven surfaces were tested in this study, as listed in Table 1. One was a smooth cast acrylic surface. The other six were rough surfaces. Three surfaces were covered with wet/dry sandpaper. These included 80, 24 and 12 grit sandpaper. The three remaining were covered with woven mesh with pitch to diameter ratios of 6.25 for M1, 4.58 for M2 and 8.45 for M3. The test fixture is the same as that used by Schultz and Flack (2003, 2005). The forward most 200 mm of the plate is covered with 36-grit sandpaper to trip the developing boundary layer. The use of a strip of roughness was shown by Klebanoff and Diehl (1951) to provide effective boundary layer thickening and a fairly rapid return to self-similarity. The test specimen mounts flush into the test fixture and its forward edge is located immediately downstream of the trip. The boundary layer profiles presented here were taken 1.35 m downstream of the leading edge of the test fixture. Profiles taken from 0.90 m to the measurement location confirmed that the flow had reached self-similarity. The upper wall of the test section was adjusted to counteract the physical growth of the boundary layer in order to maintain zero pressure gradient. A schematic of the water tunnel test fixture is shown in Figure 1.

Velocity measurements were made using a TSI FSA3500 two-component, fiber-optic laser Doppler velocimeter (LDV). The LDV used a four beam arrangement and was operated in backscatter mode. The measurement volume diameter was 90 μm, and its length was 1.3 mm. The viscous length scale (ν/u_τ) varied from 7.5 μm for the rough walls to 13 μm for the smooth wall. The diameter of the probe volume, therefore, ranged from 7 to 13 viscous lengths in the present study. The LDV probe was mounted on a Velmex three-axis traverse unit. The traverse allowed the position of the probe to be maintained to ± 5 μm in all directions. In order to facilitate two-component, near wall measurements, one of the vertical beams was redirected by a beam displacer on the LDV probe, aligning the beam parallel to the test surface. This eliminated the need for tilting or rotation of the probe as was done in previous studies in the facility (Schultz & Flack (2003) and Flack *et al.* (2005)). Velocity measurements were conducted in coincidence mode with

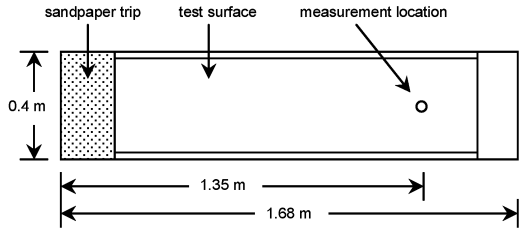

Figure 1. Test surface configuration

50,000 random samples per location. Doppler bursts for the two channels were required to fall within a 100 μs coincidence window or the sample was rejected. In order to facilitate near-wall measurements of the streamwise mean velocity on the smooth wall, beam expander optics were used to reduce the size of the measurement volume. In this case, the measurement volume diameter was 46 μm, and its length was 0.34 mm, corresponding to 3.5 and 26 viscous length scales, respectively.

In this study, the friction velocity, u_τ, for the smooth surface was found using the Clauser chart method with log-law constants κ= 0.41 and B = 5.0. This was confirmed using the measurement of velocity gradient in the linear sublayer. For the rough walls, u_τ was obtained using a procedure based on the modified Clauser chart method given by Perry and Li (1990). Data from $y^+ \geq 100$ and $y/\delta \leq 0.125$ were used. Further details of the procedure are given in Schultz & Flack (2003). The total stress method was also used to verify u_τ for all the test surfaces. This method assumes a constant stress region equal to the wall shear stress exists in the overlap and inner layer of the boundary layer. In all cases, the results from the modified Clauser chart and the total stress methods agreed well within the experimental uncertainty. Results presented throughout this paper use the friction velocity determined by the modified Clauser chart method.

UNCERTAINTY ESTIMATES

Precision uncertainty estimates for the velocity measurements were made through repeatability tests using the procedure given by Moffat (1988). Ten replicate velocity profiles were taken on both a smooth and a rough plate. LDV measurements are also susceptible to a variety of bias errors including angle bias, velocity bias, and velocity gradient bias, as detailed by Edwards (1987). These bias estimates were combined with the precision uncertainties to calculate the overall uncertainties for the measured quantities. The resulting overall uncertainty in the mean velocity is ±1%. For the turbulence quantities, $\overline{u'^2}$, $\overline{v'^2}$ and, $\overline{u'v'}$, the overall uncertainties are ±2%, ±3%, and ±7%, respectively. The uncertainty in u_τ for the smooth walls using the Clauser chart method is ±3%, and the uncertainty in u_τ for the rough walls using the modified Clauser chart method was ±5%. The increased uncertainty for the rough walls resulted mainly from the extra two degrees of freedom in fitting the log law (the location of virtual origin and the roughness function). The uncertainty in u_τ using the total stress method is ±7% for both the smooth and rough walls. The uncertainties in δ,

Table 1. Experimental Test Conditions

Surface	Symbol	U_e (m/s)	Re_θ	u_τ (m/s)	ΔU^+	δ (mm)	δ^* (mm)	θ (mm)	k (mm)	k^+	k_s^+	δ/k	δ/k_s
Smooth	--	2.00	6,140	0.0763	--	32.5	4.03	3.08	--	--	--	--	--
80-grit Sandpaper	S1	1.98	7,960	0.0917	5.24	37.2	5.86	4.21	0.690	60	36	54	91
Fine Mesh	M1	1.99	7,280	0.0981	6.31	34.8	5.73	4.05	0.320	28	56	110	55
24-grit Sandpaper	S2	1.99	8,950	0.120	10.8	37.9	7.68	4.94	1.80	200	360	21	11
Medium Mesh	M2	2.00	9,100	0.119	10.9	38.3	7.71	4.99	1.40	150	370	27	11
12-grit Sandpaper	S3	2.00	12,490	0.132	13.0	44.9	9.86	6.11	2.85	380	860	16	7.0
Coarse Mesh	M3	2.00	13,040	0.133	13.7	46.8	10.5	6.39	2.45	330	1150	19	5.5

δ^*, and θ are ±6%, ±4%, and ±5%, respectively. Note that δ reported in the present study is δ_{995}.

EXPERIMENTAL RESULTS

The experimental conditions for each test case are presented in Table 1. Substantial increases in the physical growth of the boundary layer were noted on the sandgrain and woven mesh rough surfaces as compared to the smooth wall. The 80-grit sandpaper showed increases of 14%, 45%, and 37%, while the 24-grit sandpaper had increases of 17%, 91%, and 60%, and the 12-grit sandpaper had increases of 38%, 145%, and 98% in δ, δ^*, and θ, respectively. The fine mesh showed increases of 7%, 42%, and 31%, while the medium mesh had increases of 18%, 91%, and 62%, and the coarse mesh had increases of 44%, 161%, and 107% in δ, δ^*, and θ, respectively.

Figure 2 shows the mean velocity profiles for the seven surfaces plotted in inner variables. The smooth wall results of DeGraaff & Eaton (2000) are shown for comparison. Both rough surfaces display a linear log region that is shifted by ΔU^+ below the smooth profile indicating an increased momentum deficit on these surfaces. The sandgrain and mesh surface produced roughness functions ranging from $\Delta U^+ = 5.2$ to 13.7, as listed in Table 1. This represents flows in the transitionally rough to fully rough flow regimes. It is of note that similar roughness functions are obtained for the mesh and sandgrain surfaces at nominally the same unit Reynolds number even though the roughness heights, k, differ substantially. This is most evident for the 80 grit sandpaper and fine mesh. The fine mesh produces a roughness function 20% larger than the sandpaper although the roughness height of the sandpaper is more than twice that of the mesh. This clearly reinforces that the roughness height alone is not a good indicator of roughness function. The roughness functions become more closely a function of roughness height for the larger roughness. The equivalent sand roughness height, k_s, defined as the uniform sand roughness height that gives that same roughness function in the fully rough regime (Nikuradse 1933), is also listed in Table 1. Schultz & Flack (2005) have previously estimated the extent of the roughness sublayer to be $5k_s/\delta$. Figure 3 shows near-wall measurements of the mean velocity for the smooth wall. The present results follow $U^+ = y^+$ well for $y^+ \leq 5$, and u_τ determined from the slope of the linear sublayer agrees with that from the Clauser chart to within 1%.

The mean velocity profiles for all test cases are presented in defect form in Figures 4 and 5. Again, shown for comparison are the smooth wall results of DeGraaff & Eaton (2000). Figure 4 shows the results using classic

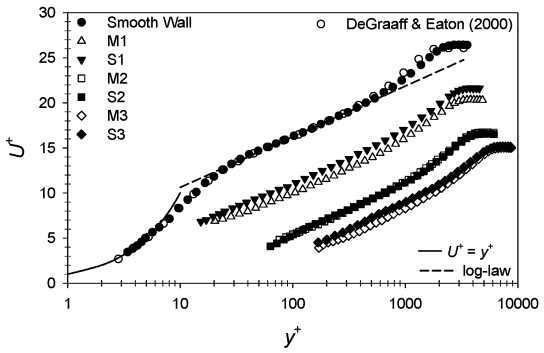

Figure 2. Mean velocity profile

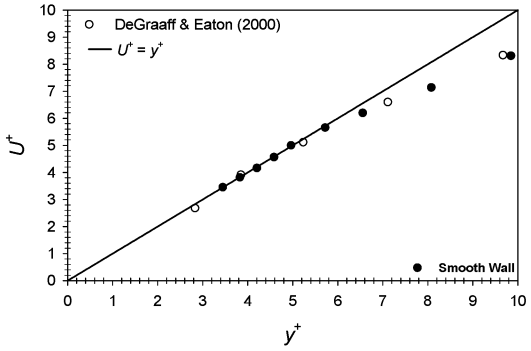

Figure 3. Near-wall smooth wall velocity measurements

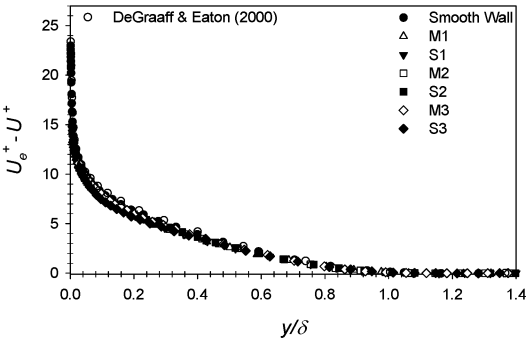

Figure 4. Velocity profile in defect form, classic scaling

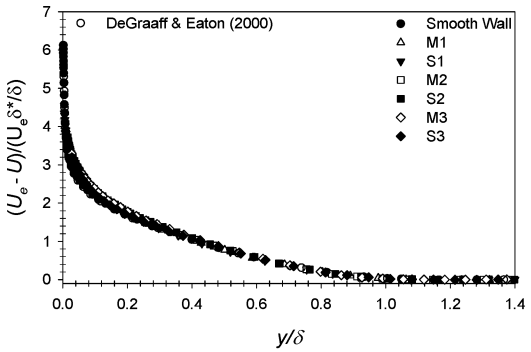

Figure 5. Velocity profile in defect form, Zagarola & Smits (1998) scaling

scaling with normalization by u_τ. Excellent collapse of the present smooth and rough wall results is seen in the outer part of the boundary layer. Figure 5 shows the velocity defect normalized using the Zagarola & Smits (1998) velocity scale, $U_e\delta^*/\delta$. Excellent collapse of both the present results and those of DeGraaff & Eaton (2000) is seen using this alternative scaling. These results indicate that similarity in the outer layer mean flow is largely insensitive to surface condition.

The normalized Reynolds stress profiles ($\overline{u'^2}/u_\tau^2$, $\overline{v'^2}/u_\tau^2$, and $-\overline{u'v'}/u_\tau^2$) for the test surfaces are presented in Figures 6-8. Also shown for comparison are the smooth wall results of DeGraaff & Eaton (2000). The streamwise Reynolds normal stresses, $\overline{u'^2}/u_\tau^2$, (Figure 6) for the smooth and rough wall show excellent agreement throughout outer region of the boundary layer. Near the wall ($y/\delta \leq 0.05$), $\overline{u'^2}/u_\tau^2$ is significantly lower on the rough walls. This suppression in $\overline{u'^2}/u_\tau^2$ increases with increasing roughness height. It is observed as a suppressed peak in the roughness sublayer for flows in the transitionally rough regime as compared to that observed in the buffer layer on a smooth wall. For flows in the fully rough regime, the near-wall peak in $\overline{u'^2}/u_\tau^2$ appears absent entirely. The region of the roughness influence

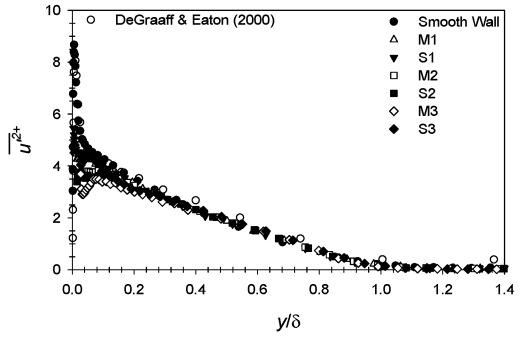

Figure 6. Axial Reynolds normal stress

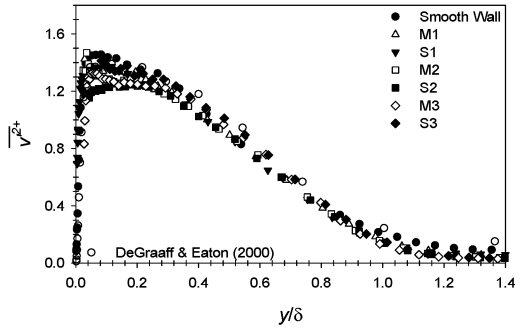

Figure 7. Wall-normal Reynolds normal stress

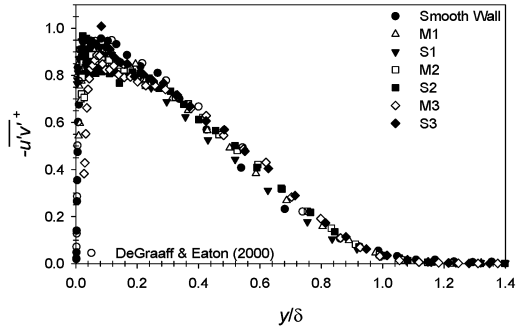

Figure 8. Reynolds shear stress

corresponds to $y \leq 3k_s$ for M1, M2, S2, M3 and S3 and $y \leq 4k_s$ for the finest sandpaper, S1.

The wall-normal Reynolds normal stresses, $\overline{v'^2}/u_\tau^2$, (Figure 7) also indicate good collapse in the outer region of the boundary layer. This result is in agreement with a number of studies, including Ligrani & Moffat (1986), Perry & Li (1990), Schultz & Flack (2003, 2005), and Flack *et al.* (2005). In the present study, the agreement in $\overline{v'^2}/u_\tau^2$ is observed for $y \geq 4k_s$ for all rough surfaces. The studies of Krogstad *et al.* (1992) and Keirsbulck *et al.* (2002) showed that significant increases in the wall-normal Reynolds normal stress penetrate well into the outer layer over rough walls with k_s/δ = 15 and 7, respectively, values

similar to the larger mesh and sandpaper roughness of the present study.

The normalized Reynolds shear stress ($-\overline{u'v'}/u_\tau^2$) profiles are presented in Figure 8. Good collapse of the profiles is observed across almost the entire boundary layer ($y \geq 3k_s$). Once again, outer layer similarity exists outside the roughness sublayer. These results provide support for Townsend's Reynolds number similarity hypothesis for uniform three-dimensional roughness in flows where k and k_s are a significant fraction of δ. Based upon these findings, even comparatively large roughness elements that have a significant effect on the mean flow, can be considered a small perturbation to the boundary layer with regards to the outer layer.

CONCLUSION

Results show that the mean velocity profiles for rough and smooth walls collapse well in velocity defect form in the outer region of the boundary layer using both classic and Zagarola & Smits (1998) scaling. The Reynolds stresses for the six rough surfaces agree well throughout most of the boundary layer and collapse with smooth wall results outside a roughness sublayer of 3 - 4k_s. Collapse had been observed in previous studies for milder roughness, however, results from the present study extend these conclusions for larger roughness heights. Outer layer similarity appears to be very robust and may exist outside the roughness sublayer for even larger roughness heights. There does not appear to be a critical value of δ/k or δ/k_s where outer layer similarity fails. Instead changes to turbulent structure appear to be confined to the roughness sublayer, even for very large roughness. Therefore, changes to the turbulence in the outer layer may only be expected if the roughness sublayer extends beyond the inner layer. These conclusions apply to rough wall boundary layers that have reached streamwise self-similarity. Boundary layers adjusting to a change in surface condition (Antonia & Luxton, 1971) may display modifications in turbulence structure into the outer layer.

REFERENCES

Antonia, R.A. and Krogstad, P.-Å. (2001), Turbulence structure in boundary layers over different types of surface roughness", *Fluid Dynamics Research*, Vol. 28, pp. 139-157.

Antonia, R.A. and Luxton, R.E. (1971), "The Response of a Turbulent Boundary Layer to a Step Change in Surface Roughness Part 1. Smooth to Rough", *Journal of Fluid Mechanics*, Vol. 48, Pt. 4, pp. 721-761.

Bandyopadhyay, P.R. (1987), "Rough-Wall Turbulent Boundary Layers in the Transition Regime", *Journal of Fluid Mechanics*, Vol. 180, pp. 231-266.

Colebrook, C.F. and White, C.M. (1937). "Experiments with Fluid Resistance in Roughened Pipes", *Proceedings of the Royal Society*, 161A, pp. 376-381.

Edwards, R.V., (1987) "Report of the Special Panel on Statistical Particle Bias Problems in Laser Anemometry", *Journal of Fluids Engineering* Vol. 109, pp. 89-93.

DeGraaff, D.B. and Eaton, J.K., (2000) "Reynolds-Number Scaling of the Flat-Plate Turbulent Boundary Layer", *Journal of Fluid Mechanics*, Vol. 422, pp. 319-346.

Flack, K.A., Schultz, M.P, and Shapiro, T.A. (2005), "Experimental Support for Townsend's Reynolds Number Similarity Hypothesis on Rough Walls", *Physics of Fluids*, Vol. 17.

Hama, F.R. (1954), "Boundary-Layer Characteristics for Smooth and Rough Surfaces", *Transactions SNAME*, Vol. 62, pp. 333-358.

Jiménez, J. (2004), "Turbulent Flows over Rough Walls", *Annual Review of Fluid Mechanics*, Vol. 36, pp. 173-196.

Keirsbulck, L., Labraga, L., Mazouz, A., and Tournier, C. (2002), "Surface Roughness Effects on Turbulent Boundary Layer Structures", *Journal of Fluids Engineering*, Vol. 124, pp. 127-135.

Klebanoff, P.S. and Diehl, F.W.,(1951) "Some Features of Artifically Thickened Fully Developed Turbulent Boundary Layers with Zero Pressure Gradient", *NACA TN* 2475.

Krogstad, P.-Å and Antonia, R.A. (1994), "Structure of Turbulent Boundary Layers on Smooth and Rough Walls", *Journal of Fluid Mechanics*, Vol. 277, pp. 1-21.

Krogstad, P.-Å, Antonia, R.A. and Browne, L.W.B. (1992), "Comparison Between Rough- and Smooth-Wall Turbulent Boundary Layers", *Journal of Fluid Mechanics*, Vol. 245, pp. 599-617.

Ligrani, P.M. and Moffat, R.J. (1986), "Structure of Transitionally Rough and Fully Rough Turbulent Boundary Layers", *Journal of Fluid Mechanics*, Vol. 162, pp. 69-98.

Moffat, R.J., (1988) "Describing the Uncertainties in Experimental Results", *Experimental Thermal and Fluid Science*, Vol. 1, pp. 3-17.

Nikuradse, J. (1933), "Laws of Flow in Rough Pipes", *N.A.C.A. Technical Memorandum 1292*.

Perry, A.E. and Chong, M.S. (1982), "On the Mechanism of Wall Turbulence", *Journal of Fluid Mechanics*, Vol. 119, pp. 173-217.

Perry, A.E. and Joubert, P.N. (1963), "Rough-Wall Turbulent Boundary Layers", *Journal of Fluid Mechanics*, Vol. 37, pp. 383-413.

Perry, A.E. and Li, J.D. (1990), "Experimental Support for the Attached-Eddy Hypothesis in Zero-Pressure Gradient Turbulent Boundary Layers", *Journal of Fluid Mechanics*, Vol. 218, pp. 405-438.

Perry, A.E., Lim, K.L., and Joubert, P.N. (1969), "Rough Wall Turbulent Boundary Layers", *Journal of Fluid Mechanics*, Vol. 37, pp. 383-413.

Raupach, M.R., Antonia, R.A., and Rajagopalan, S. (1991), "Rough-Wall Boundary Layers", *Applied Mechanics Review*, Vol. 44, No. 1, pp. 1-25.

Schlichting, H. (1979), *Boundary-Layer Theory*, 7th Edition, McGraw-Hill, New York.

Schultz, M.P. and Flack, K.A. (2005), "Outer Layer Similarity in Fully Rough Turbulent Boundary Layers", *Experiments in Fluids*, Vol. 38.

Schultz, M.P. and Flack, K.A. (2003), "Turbulent Boundary Layers over Surfaces Smoothed by Sanding", *ASME Journal of Fluids Engineering*, Vol. 125, pp. 863-870.

Townsend, A.A. (1976) *The Structure of Turbulent Shear Flow*, 2nd Ed., Cambridge U. Press, Cambridge, UK.

Zagarola , M.V. and Smits, A.J. (1998), "Mean-Flow Scaling of Turbulent Pipe Flow", *Journal of Fluid Mechanics*, Vol. 373, pp. 33-79.